Miller, D. N., "Scale-Up of Agitated Vessels Gas-Liquid Mass Transfer," *AIChE J.*, 20, 445 (1974).

Ramakrishnan, S., Kumar, R., Kuloor, N. R., "Studies in Bubble Formation Under Constant Flow Conditions," *Chem. Eng. Sci.*, 24, 731 (1969).

Reitema, K., and Ir. S. P. P. Ottengraf, "Laminar Liquid Circulation and Bubble Street Formation in a Gas Liquid System," *Trans. Inst. Chem. Engrs.*, 48, T54 (1970).

Robinson, C. W., and C. R. Wilke, "Oxygen Absorption in Stirred Tanks: A Correlation for Ionic Strength Effects," *Biotechnol. Bioeng.*, 15, 755 (1973).

Towell, G. D., C. P. Strand, and G. H. Ackerman, "Mixing and Mass Transfer in Large Diameter Bubble Columns," *AIChE Symposium Series No. 10* (1965).

Van Krevelen, D. W., and P. J. Hoftijzer, "Studies of Gas Bubble Formation," *Chem. Eng. Progr.*, 46, 29 (1950).

Yagi, H., and F. Yoshida, "Oxygen Absorption in Fermentors—Effects of Surfactants, Antifoaming Agents, and Sterilized Cells," *J. Ferm. Technol.*, 52, 905 (1974).

Yoshida, F., and K. Akita, "Performance of Gas Bubble Columns," *AIChE J.*, 11, 9 (1965).

Zlokarnik, M., "Influence of some Important Geometric, Material and Process Parameters on Mass Transfer in Gas-Liquid Contacting," paper presented at Engineering Foundation Conference, Henniker, N.H. (1977).

Manuscript received August 1, 1977; revision received November 21, and accepted December 7, 1977.

Cold Flow Mixing Rate Data for Pulverized Coal Reactors

VINCENT J. MEMMOTT

and

L. DOUGLAS SMOOT

Department of Chemical Engineering
Brigham Young University
Provo, Utah 84602

Mixing rates of particles and gases in confined, coaxial jets are reported for tests with conditions simulating those of pulverized coal gasification and combustion processes. Gas velocity, particle mass flux, and gas composition were measured at various radial and axial locations downstream of the primary jet exit plane. Effects of inlet velocity, density, injection angle, particle loading level, and particle size on the rates of mixing were determined. Increasing injection angle and secondary velocity significantly increased gas and particle mixing rates, while effects of other variables were much less significant. Dispersion of particles lagged that of the gas in all cases investigated.

SCOPE

Many chemical processes involve the heterogeneous mixing of gas and particulate phases. Examples of such processes are fluidized, heterogeneous, catalytic systems; pulverized coal combustors; entrained coal gasifiers; MHD power generators; and air breathing missiles. A common method of contacting the particles and the gases is to inject them from separate jets into a mixing zone. The jets may be free (exhausting into an unconfined environment) or confined by the walls of the system. Considerable effort has been expended to investigate mixing of gaseous free and confined jets. Extensive literature reviews of turbulent mixing in parallel systems have been reported by Tufts and Smoot (1971), Harsha (1971), Stowell and Smoot (1973), and Hedman and Smoot (1975). Several experimental investigations have been conducted at this laboratory to determine turbulent mixing characteristics in parallel and nonparallel coaxial jet systems. Smoot and Allred (1975) and Smoot and Fort (1976) have reported particle and gas mixing data with nonparallel injection. Smoot (1976) has summarized and correlated the experimental turbulent mixing data previously obtained at this laboratory together with data from several independent investigations.

Only limited data have been reported for experimental investigations, where the secondary-primary velocity ratio was near unity or for jets containing particles. Both are characteristic of pulverized coal combustion and gasification. Studies of Fejer et al. (1967), Beasley et al. (1970), and Durao et al. (1973) consider a primary velocity near that investigated in this study. However, these three sets of tests were performed with air containing no trace gas or particles, and only velocity data were reported. Only Beasley (1970) considers a nonparallel system with primary/secondary velocities of comparable magnitude, but without particles. No studies have been located where mixing with nonparallel injection was investigated under conditions similar to this study.

The purpose of this research was to experimentally investigate the mixing characteristics of particle laden, confined jets under conditions that would simulate industrial pulverized coal furnaces and entrained gasifiers. Radial profiles for gas composition, particle mass flux, and gas velocity were measured at various axial locations in the mixing chamber. Effects of velocity, density, injection angle, particle loading level, and particle size on the rates of particle and gas mixing were examined.

Air, argon, and silicon particles comprised the primary stream. The secondary air stream was heated with an electric circulation heater. Mixing experiments were conducted at two ratios of secondary to primary density (0.6 and 0.8) and velocity (1.3 and 2.0). Tests were also conducted at 0, 40, and 60% solids by weight in the primary jet and with three different particle size distributions. Fifty five tests were completed, of which six were conducted without particles.

Vincent J. Memmott is with Exxon Corporation, Baytown, Texas.

0001-1541-78-1140-0466-$01.05.

The data resulting from these tests can be used to evaluate mixing characteristics in combustion systems, to determine turbulent mixing parameters for nonreacting systems containing particles, and to evaluate particle-gas mixing models. The results may also be useful in design and control of furnaces and gasifiers.

CONCLUSIONS AND SIGNIFICANCE

Experimental measurements were made of radial profiles for velocity, argon composition, and particle mass flux in a confined jet system. Logarithmic center line axial decay plots were made from these experimental data. Resulting conclusions were:

1. Primary and secondary gases mixed faster than the particles in all cases, with the ratio of gas to particle mixing rates ranging from about 2 to 6.
2. Mixing was generally about two times faster in the nonparallel injector system than in the parallel injector system for both particles and gases.
3. An increase in the secondary velocity caused an increase in the gas mixing rates. Gas mixing rates with higher secondary velocities were about twice those observed for the lower secondary velocity.
4. An increase in particle solids loading had very little effect on particle or gas mixing rates using the nonparallel injector system; however, particle mixing rates were decreased with solids loading increases in the parallel injector system, while gas mixing rates were increased.
5. Reducing density of the secondary stream caused very little change in mixing rates in the nonparallel system, while the mixing rates seemed to decrease by a factor of approximately 1.2 to 1.3 in the parallel system, although these differences were not significant.
6. Smaller particles dispersed more rapidly than larger particles, by factors of 1.5 to 2.5.
7. Little correlation was observed between gas and particle mixing rates in the parallel system. Changing flow conditions significantly affected the gas mixing rate, while much less effect was generally observed in the particle mixing rate.
8. A significant correlation between particle and gas mixing rates was observed for the nonparallel injector system, with changes in gas mixing rate accompanied by similar changes in particle mixing rate.

These test results are the only known particle and gas mixing data for experimental systems that simulate the operation of pulverized coal combustors and entrained gasifiers. The effects of selected variables on the gas and particle mixing rates provide information for modeling of mixing rates. This information also suggests potential methods for control of the mixing process by adjusting operating variables.

EXPERIMENTAL PROGRAM

The specific objective of this test program was to determine the effects of inlet stream condition and injection angle on the rates of turbulent mixing of particles and gases in a confined duct. Although the purpose of this study was to simulate the operating conditions in pulverized coal reactors, tests were conducted in the absence of chemical reaction, and silicon powder was used in place of pulverized coal.

Seven sets (1 to 7) of inlet stream conditions were selected to simulate the operating conditions of typical pulverized coal furnaces and gasifiers and are summarized in Table 1. Summaries of operating conditions in some pulverized coal combustors and gasifiers were reported by Thurgood et al. (1976) and Skinner et al. (1976); these summaries have provided a basis for selecting operating conditions for this study. The velocity of the primary jet was about 30.5 m/s for all flow tests, while the secondary velocity was either about

TABLE 1. SUMMARY OF DESIGN TEST CONDITIONS

Test condition No.	1	2	3	4	5	6	7
Primary							
Velocity, m/s	30.5	30.5	30.5	30.5	30.5	30.5	30.5
Temperature, °K	283	283	283	283	283	283	283
Particle size*	std.	std.	std.	std.	small	large	—
Flow rate, g/s							
Air	5.4	5.4	5.4	5.4	5.4	5.4	5.4
Argon	17.4	17.4	17.4	17.4	17.4	17.4	17.4
Particles	15.2	34.2	15.2	15.2	15.2	15.2	0
% solids loading	40.0	60.0	40.0	40.0	40.0	40.0	0
% (mole) argon	70.0	70.0	70.0	70.0	70.0	70.0	70.0
Secondary							
Injection angle, deg	0, 30	0, 30	0, 30	0, 30	0, 30	0, 30	0, 30
Velocity, m/s	38.1	38.1	61.0	38.1	38.1	38.1	38.1
Temperature, °K	283	283	283	370	283	283	283
Sec/pri ratios							
Velocity	1.3	1.3	2.0	1.3	1.3	1.3	1.3
Gas density	0.8	0.8	0.8	0.6	0.8	0.8	0.8
Total density	0.47	0.32	0.47	0.10	0.47	0.47	0.47
Gas flow	20.0	20.0	32.0	15.5	20.0	20.0	20.0
Total flow	12.0	8.0	19.2	9.3	12.0	12.0	12.0
No. of tests for this condition†	3, 6	3, 4	5, 3	3, 6	3, 5	4, 4	3, 3

* Standard particle size, d_m = 38.6 μm, small particle size, d_m = 19.0 μm, large particle size, d_m = 54.1 μm. See Table 2 for size distributions.
† At different axial stations and reproduced tests; first number is for parallel injection, while the second number is for nonparallel injection.

TABLE 2. PARTICLE SIZE DISTRIBUTIONS* OF SILICON AND PULVERIZED COAL

Mean of size increment, μm	Small silicon, wt. %	Standard silicon, wt. %	Large silicon, wt. %	Mean of size increment, μm	Bituminous coal,† wt. %
				2.83	0.25
				3.56	0.43
				4.49	0.54
5.70	0.83	0.00	0.00	5.66	0.76
7.20	1.09	0.01	0.00	7.13	1.26
9.00	2.85	0.04	0.00	8.98	2.06
11.40	7.41	0.11	0.01	11.31	3.17
14.35	14.80	0.27	0.03	14.25	4.30
18.10	20.76	0.72	0.08	17.96	6.03
22.80	17.88	1.91	0.23	22.63	8.11
28.70	12.78	4.95	0.69	28.51	10.06
36.15	8.06	11.89	5.12	35.92	11.87
45.55	8.06	18.40	15.31	45.26	11.89
57.40	2.26	20.76	25.15	57.02	12.06
72.30	1.06	29.87	35.25	71.84	10.71
91.10	2.15	11.07	18.11	85.17	6.15
—	—	—	—	≧90	9.75
Mass mean diameter, μm	19.0	38.6	54.1	—	47.3**

* From Coulter counter measurements.
† Pulverized coal, 70% through 200 mesh supplied by Utah Power and Light, Salt Lake City, Utah.
** Assuming 110 μm size for 9.75% of coal > 90 μm.

37 or 61 m/s. The secondary jet temperature was either 285° or 370°K.

Silicon powder was chosen for this study because the bulk density and size distribution were similar to those of pulverized coal. However, the silicon particles are spherical. Some of the silicon powder was divided into a small diameter cut and a large diameter cut using a cyclone particle classifier. The mass mean diameters of the three size distributions tested were 19.0, 38.6, and 54.1 μm. The size distributions for these test particles are shown in Table 2, where comparison with a typical pulverized coal is also shown. The solids loading of the particles in the primary jet was usually 40 mass % but was increased to 60% in selected tests. The injection angle of the secondary jet was either 0 or 30 deg, with respect to the primary jet. Fifty five tests were completed; six of these tests were conducted without particles in the primary jet.

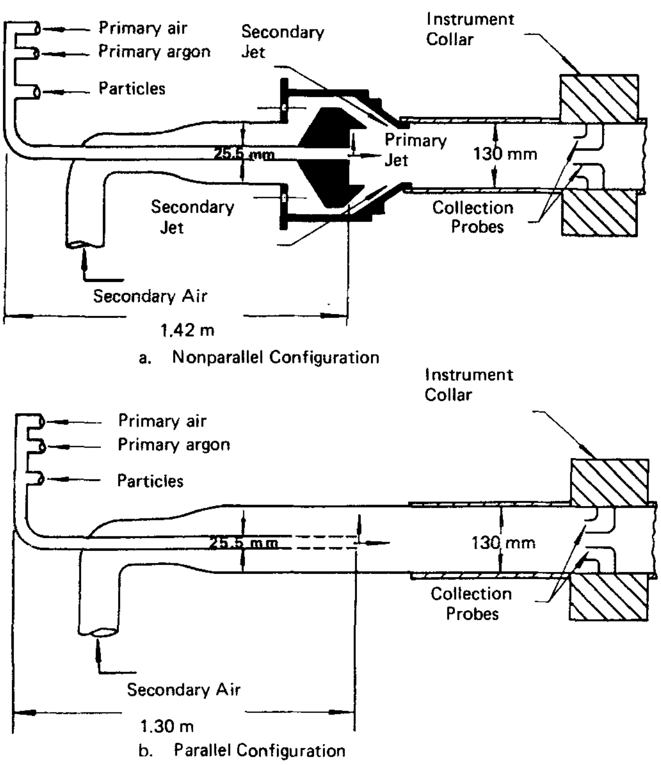

Fig. 1. Schematic diagrams of nonparallel and parallel jet systems.

TEST FACILITY AND INSTRUMENTATION

The test facility shown schematically in Figure 1 was adapted for parallel and nonparallel (30 deg) secondary injection tests. The inlet flow areas of both the primary and secondary jets were the same for the parallel and nonparallel systems. The 25.5 mm diameter primary jet was composed of a two-phase mixture of argon, air, and the small silicon particles. The secondary jet consisted of air that could be electrically heated.

Gas and particle samples were taken with isokinetic collection probes, and gas velocities were obtained from the measured static and stagnation pressures. Eight collection and eight stagnation probes were located so that radial profile data were collected in two perpendicular lines across the duct. Tests were ordinarily made at four different axial stations. Argon composition was determined by gas chromatographic analysis. Particle mass flux was determined from the weight of a particle sample collected during a timed interval in a ceramic filter. Gas flow rates of the primary and secondary jets were determined from pressure and temperature measurements and throat areas of the flow control nozzles. The particle feeder was calibrated and preset for each test. Static and stagnation pressures in the probe collar were measured on a 2.5 m manometer board.

DATA REDUCTION

To minimize the errors introduced by jet and instrument collar misalignment and other data scatter, the radial gas and particle mixing data were statistically fitted using nonlinear least-squares techniques (Hedman and Smoot, 1975) as illustrated in Figure 2 for argon. Figure 2 also presents the argon composition profiles for one reproduced test at (z/r_1) of 24. Data points are shown in Figure 2 for two of the four axial stations. The duplicate data points at a radial location of 12.7 mm (1.0 r/r_1) from the center line, but at different annular locations, show good symmetry in the test mixing section.

Similar agreement was obtained between the empirical curve fit and the gas and particle data for most of the tests. The curve fitted radial profiles obtained for the argon composition and the particle mass flux were used for basic data comparisons.

Eight tests were reproduced, and the average difference in the reproduced tests for the center line data was 7.3% for the argon composition and 10.5% for the particle mass flux. Three independent mass flow balances were computed for all tests by integrating the empirical curve fit of the radial profile data for particle mass flow rate, total gas flow rate, and argon mass flow rate, and comparing the results with known feed rates for particles, argon, and total gas. Of the 157 material balance comparisons computed for the fifty-five tests, thirty-eight were found to be in error by more than ±15%. Much of this error was introduced by the difficulty of measuring the low velocity levels with a stagnation probe. For the case of the smaller particles, the particle material balances were consistently low because of problems in accurately collecting particle samples. For tests with low secondary density and high secondary velocity, the argon material balance was consistently high. Under these conditions, a large error in the material balance resulted from a small error in the measured velocity. Three of the experiments were discarded owing to large material balance errors. For the fifty-two tests with material balance errors less than 15%, an average absolute error of less than 10% occurred for the particles, 5.9% for the argon and 6.7% for the total gas.

In order to discuss rates of mixing in conjunction with the center line axial decay plots, two important definitions are presented. The core length is the distance from the exit plane ($z/r_1 = 0$) to the point where the decay line intercepts the normalized concentration of 1.0 as illustrated in Figure 3. The core length is thus the length from the primary jet exit plane to the last point where the original composition of the primary stream still exists at the jet center line. Smoot and Purcell (1967) have shown that this core length is inversely proportional to a parameter known as the mixing coefficient for coflowing, parallel, free jet systems. In the discussion that follows, the term rate of mixing is defined to be proportional to the mixing coefficient and thus inversely proportional to the core length.

The second important term is the decay slope, or the slope of the logarithmic line fitted to the data in the center line axial decay plot. The slope of this line is called the rate of decay, which is not necessarily a function of the rate of mixing (Stowell and Smoot, 1973). The axial decay plots in Figures 3 through 8 indicate that the decay slopes do not change greatly as a function of injection angle or flow conditions, while the core length often changes markedly. Smoot and Allred (1975) and Hedman and Smoot (1975) have also shown that the rate of decay is not a strong function of mixing rate for parallel and nonparallel systems.

DATA ANALYSIS

Table 3 summarizes statistically determined core length and decay slope values for all tests. Center line decay data for nearly all of the tests are shown in Figures 3 through 8. Data in the figures from tests with high material balance errors are marked (+). The figures also show the normalized values of the completely mixed argon concentration $(w_c/w_1)_m$ and particle mass flux $(M_c/M_1)_m$. Detailed radial profiles for all tests are reported by Memmott (1977), together with methods for statistical analysis of the core lengths and the decay slopes. Observations from these data follow.

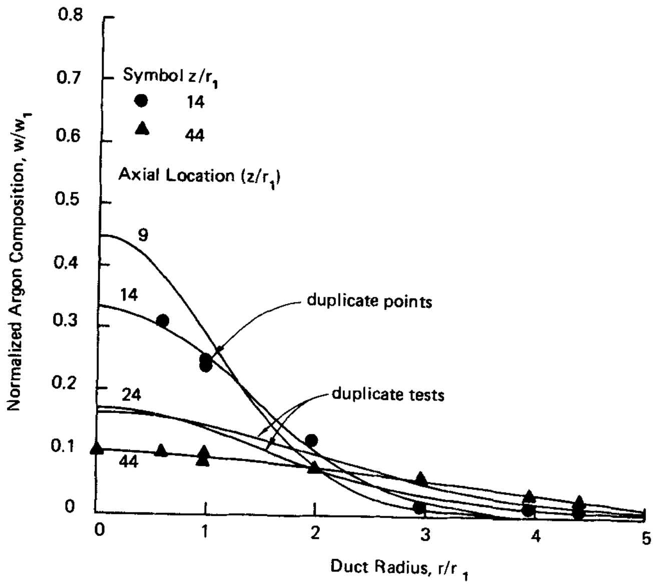

Fig. 2. Example of empirical curve fit with data for test condition 1 at 30 degree secondary injection angle.

Gas vs. Particles Mixing Rates

In all of the tests conducted, particles dispersed at a much slower rate than the gases. An effort was made to insure that the gases and particles were well mixed and at near equal velocities at the exit plane of the primary jet. However, from that point, even the smallest particles dispersed much more slowly than the gases. Since the core length is inversely proportional to the mixing coefficient, the gas mixing rate was thus determined from the data of Table 3 to be two to six times that of the particle dispersion rate. This factor was similar for parallel or nonparallel injection as illustrated in Figures 3 to 5. Even for the smallest mean particle size studied (19 μm), gas mixing was about twice that of the particles. Major causes of particle dispersion are thought to be particle drag due to turbulent motion of the gas and mean drag between particles and gas. With either of these particle dispersion processes, smaller particles are excepted to disperse more rapidly owing to their lower inertia. Hedman and Smoot (1975) have shown theoretically that the former mechanism was dominant for a somewhat different set of test results conducted earlier at this laboratory.

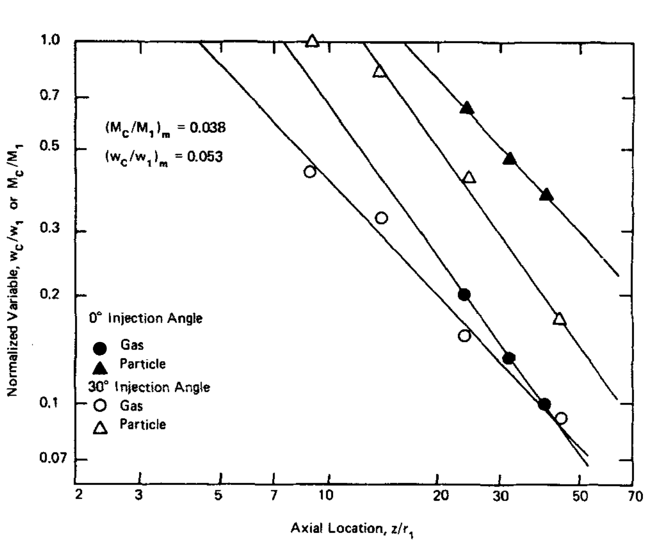

Fig. 3. Argon and particle center line decay data for test condition 1.

Table 3. Summary of Core Length and Decay Slope Values for All Tests

	Flow condition (Table 1)	Core length, cm	Core length interval,† cm	Slope/interval†,**
A. 30 deg injection				
1. Gas parameters	1	5.5	4.7-6.4	−1.1 (0.10)
	2	5.9	5.4-6.5	−1 1 (0.06)
	3	2.9	2.9-2.9	−1.0 (0.00)
	4	5.1	4.6-5.5	−1.0 (0.06)
	5	3.7	2.6-4.7	−0.9 (0.12)
	6††	8.3		−1.7
	7	6.0	5.3-6.8	−1.5 (0.15)
2. Particle parameters	1	15.7	13.3-17.8	−1.4 (0.21)
	2	15.1	13.2-16.8	−1.2 (0.16)
	3	9.2	4.7-12.1	−1.2 (0.59)
	4	14.6	13.1-15.9	−1.5 (0.18)
	5	8.3	8.2-8.3	−1.2 (0.01)
	6	21.0	19.4-22.3	−1.6 (0.17)
B. 0 deg injection				
1. Gas parameters	1	9.5	9.0-9.9	−1.4 (0.05)
	2	5.6	0.2-12.1	−0.9 (0.57)
	3	4.4	2.1-6.9	−1.1 (0.28)
	4	11.7	11.0-12.4	−1.4 (0.06)
	5	13.6	12.0-15.0	−1.8 (0.18)
	6	13.5	11.9-15.0	−1.5 (0.14)
	7	13.4	10.0-16.2	−1.7 (0.35)
2. Particle parameters	1	20.3	19.6-21.0	−1.1 (0.05)
	2	28.1	15.1-33.3	−1.7 (1.06)
	3	25.9	23.6-27.6	−1.7 (0.27)
	4	26.9	22.7-29.8	−1.3 (0.36)
	5	18.8	5.5-25.5	−1.5 (0.90)
	6	30.4	26.0-33.7	−1.5 (0.36)

* Core length values are reported in this table in centimeters but are shown in terms z^*/r_1 in Figures 3 to 8, where $r_1 = 12.7$ mm.
† All statistical intervals were established at the 70% confidence level.
** Term in ( ) is confidence interval; that is, $-1.1\,(0.10) = -1.1 \pm 0.10$.
†† No statistical confidence interval could be established for this case owing to lack of data.

Effect of Injection Angle

Increasing the angle of injection of the secondary jet with respect to the primary jet from 0 to 30 deg (see Figure 1) significantly increased the rate of mixing of the gases and the particles. Depending upon other test conditions, mixing rates of both gases and particles were about twice as fast with the nonparallel injection as with the parallel injection. Particle dispersion rates were accelerated to about the same extent as gas mixing rates by injecting on an angle of 30 deg, as illustrated by Table 3 and in Figures 3 to 5. This result suggests that significant control of the mixing process can be achieved through control of the injection angle. Injecting the secondary stream at an angle of 30 deg increases convective mixing between the two jets but may decrease turbulent shear forces. Previous results (Smoot and Allred, 1975) for somewhat different test conditions have suggested that 60 deg injection may be near optimum to promote maximum mixing. A complete theoretical explanation of the interaction of these forces in such a complex flow has not been available.

Effect of Secondary Velocity

Many pulverized coal combustors and entrained gasifiers operate with a primary velocity near 30 m/s in order

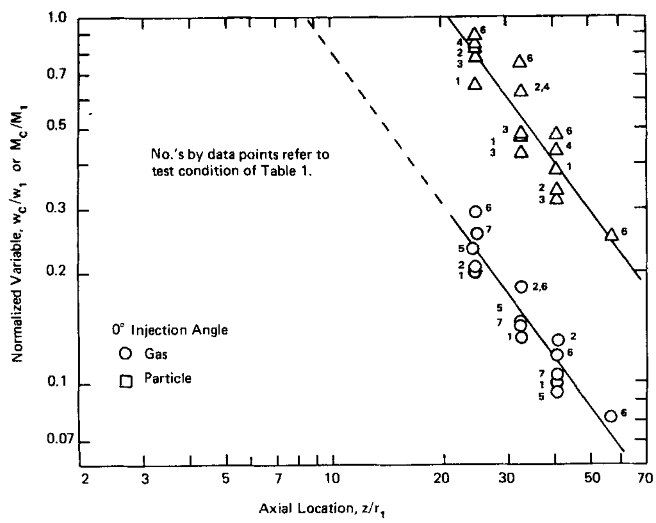

Fig. 4. Effects of solids loading level, gas density, secondary velocity, and particle size on mixing rates of gas and particles (0 deg injection).

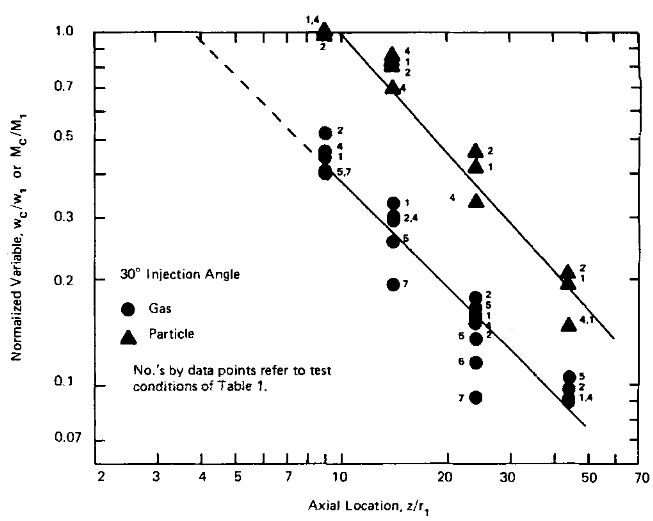

Fig. 5. Effects of solids loading level, gas density, secondary velocity, and particle size on mixing rates of gas and particles (30 deg injection).

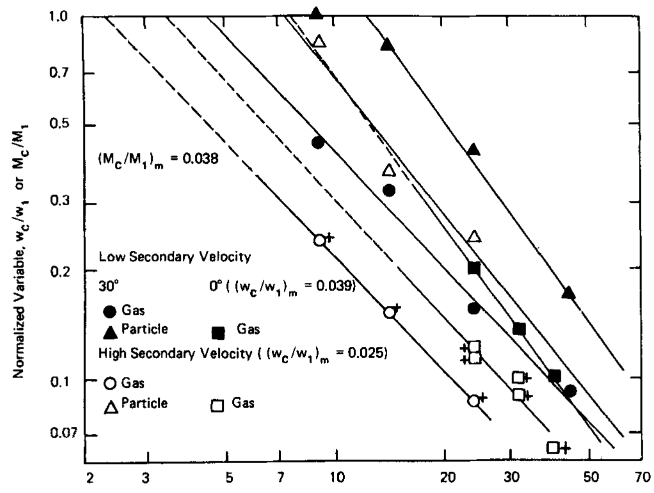

Fig. 6. Effect of secondary velocity on gas and particle center line decay.

TABLE 4. EFFECT OF SECONDARY VELOCITY ON RELATIVE JET MIXING RATES

(RECIPROCAL CORE LENGTH, m^{-1})

Case	0 deg injection Gas	0 deg injection Particle	30 deg injection Gas	30 deg injection Particle
1 (Low sec. vel.)	10.6	4.9	18.1	6.4
3 (High sec. vel.)	22.7	3.9	34.0	10.7

to minimize erosion. Secondary velocities can be somewhat greater when the secondary stream does not contain particles. In selected tests, the velocity of the secondary air was increased from 38 to 61 m/s. As illustrated in Figure 6 and summarized in Table 4, gas mixing rates (reciprocal core lengths) were approximately doubled for either 0 or 30 deg secondary injection. However, particle dispersion was not increased with increasing velocity using parallel secondary injection (see Figure 4) and was somewhat less than gases for nonparallel secondary injection. When primary and secondary velocities are nearly equal, turbulent shear stresses and thus mixing rates in parallel coaxial systems are greatly reduced. It is therefore not surprising that an increase in the secondary velocity, which increases the difference in the primary and secondary velocity, leads to higher turbulent stresses and high jet mixing rates. Control of secondary velocity is another parameter that can be effectively used to control the mixing processes in these types of combustion systems, especially for the gases.

Effect of Solids Loading

In many pulverized coal furnaces and gasifiers, solids loading levels of 40 to 90 mass % are typical. In these tests, the mass percentage of solid particles in the primary jet was varied from 0 to 60%. Over the entire range studied, neither gas nor solid mixing rates were significantly altered by the presence of the particles at either level investigated for nonparallel injection. Gas mixing rates seemed to be enhanced somewhat with increasing percent solids, while some decrease was observed in particle dispersion rates using parallel injection. However, from Table 3, these observations are generally not significant at the 70% confidence level. Some of these observations are illustrated in Figures 4 and 5 and summarized in Table 5. Previous laboratory measurements for jets with significantly different velocities and particle sizes and up to 30 mass % of solids

TABLE 5. EFFECT OF SOLIDS LOADING ON RELATIVE JET MIXING RATES

(RECIPROCAL CORE LENGTH, m^{-1})

Case	0 deg injection Gas	0 deg injection Particle	30 deg injection Gas	30 deg injection Particle
7 (0% loading)	7.5	—	15.5	—
1 (40% loading)	10.6	4.9	18.1	6.4
2 (60% loading)	17.9	3.6	16.9	6.6

TABLE 6. EFFECT OF GAS DENSITY ON RELATIVE JET MIXING RATES

(RECIPROCAL CORE LENGTH, m^{-1})

Case	0 deg injection Gas	0 deg injection Particle	30 deg injection Gas	30 deg injection Particle
1 (High sec. density)	10.6	4.9	18.1	6.4
4 (Low sec. density)	8.5	3.7	19.8	6.9

(Hedman and Smoot, 1975; Smoot and Allred, 1975) showed little effect of solids on gas mixing rates for parallel injection.

Effects of Gas Density

In coal furnaces and gasifiers, variation of primary gas density is limited by problems in coal softening at higher temperatures; however, secondary temperatures can be varied somewhat in order to improve combustion efficiency or to otherwise alter the reaction process. Higher inlet temperatures are often limited by material problems, while lower temperatures can lead to low combustion efficiencies. In these tests, the secondary gas density was altered by increasing the inlet gas temperature from 283° to 370°K. Over this relatively small but practical variation in secondary gas density, no significant effects of particle or gas mixing rates were observed using nonparallel injection (see Figure 5 and Table 6). For parallel injection, lowering the secondary gas density by about 25% reduced gas and particle mixing rates by about 25 to 35% (see Figure 7 and Table 6). Thus, the effects of changing secondary density were not nearly as significant as changes in injection angle or secondary velocity. Reducing secondary density reduces the momentum level and thus the turbulent stress between the primary and secondary streams.

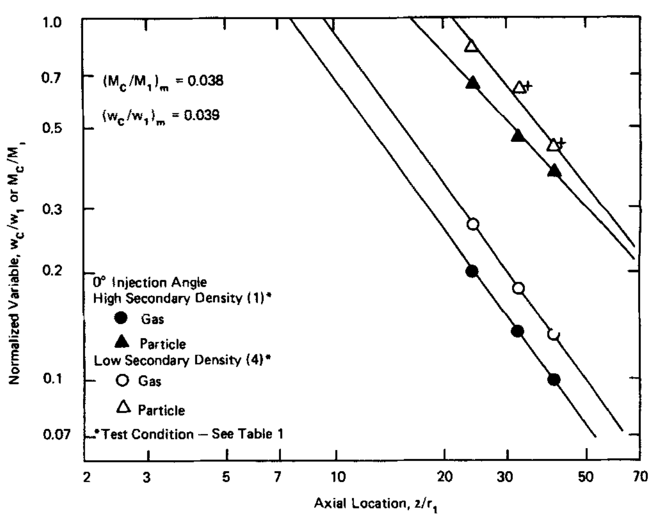

Fig. 7. Effect of secondary gas density on the rates of decay of particles and gas—0 deg injection angle.

Table 7. Effect of Particle Size on Relative Jet Mixing Rates

(reciprocal core length, m^{-1})

Case	0 deg injection Gas	0 deg injection Particle	30 deg injection Gas	30 deg injection Particle
5 (small, 19.0 μm)	7.4	5.3	27.3	12.1
1 (standard, 38.6 μm)	10.6	4.9	18.1	6.4
6 (large, 54.1 μm)	7.4	3.3	12.1	4.8

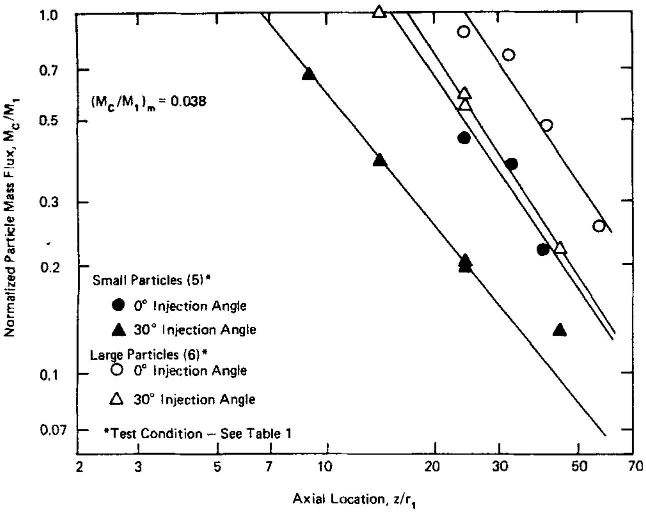

Fig. 8. Effect of particle size on the rate of decay of particles.

Effect of Particle Size

Many coal processes use finely pulverized coal, whose size is often in the range of 70% through 200 mesh. The mass mean particle size of such coals is usually in the range of 50 to 70 μm, with significant quantities of individual particle sizes in the range from 5 to over 100 μm (Table 2). In this study, three separate size distributions of silicon were examined. Mass mean

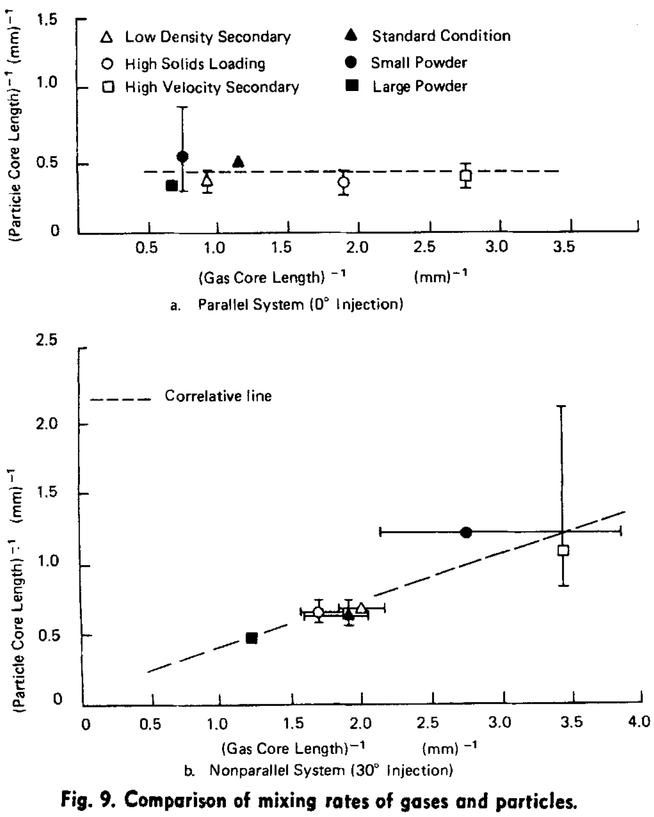

Fig. 9. Comparison of mixing rates of gases and particles.

diameters were 19.0, 38.6, and 54.1 μm. Test results in Table 7 and Figures 4 and 5 show that increasing particle size at fixed solids loading (40%) caused significant decreases in gas mixing rates for nonparallel injection but had little effect on gas mixing rates for parallel injection. Further, results of Table 7 and Figure 8 show, not surprisingly, that particle dispersion rates are dependent upon particle size. Mixing rates using the smallest particle set were about 1.5 to 2.5 times faster than those with the larger particle set, with the greater effect observed using nonparallel injection. Even the smallest particles (19.0 μm) indicate significantly slower dispersion rates than the gases.

Correlation of Particle and Gas Mixing Rates

In all cases tested, particles were observed to disperse less rapidly than the gases. A correlation of particle and gas mixing rates is shown in Figures 9*a* and *b*, where the reciprocal of the particle core length is plotted vs. the reciprocal of the gas core length for both parallel and nonparallel systems, respectively. Since the rate of mixing is inversely proportional to the core length, Figures 9*a* and *b* are essentially plots of particle mixing rate vs. gas mixing rate. Each datum point includes confidence intervals for those cases where the interval is larger than the data point.

For the parallel system, the test variables appear to have had a significant effect on gas mixing rates, but almost no effect on particle mixing rate. A statistical analysis of these data resulted in a correlation coefficient of 0.06, which indicates very little correlation between particle and gas mixing rates.

A much stronger interaction of particle and gas mixing rates was observed for the nonparallel system. Both particle mixing rates and gas mixing rates appear to be affected significantly by the test variables investigated. The correlation coefficient for these data was 0.82 ($R^2 = 0.82$), which indicates a much stronger correlation between the gas and particle mixing rates.

The relationship of gas and particle mixing rates is a strong function of injection angle, and this observation suggests a technique for independent control of gas and particle mixing rates. Such control of the mixing processes may lead to increases in combustion efficiency or to reduction in the rate of pollutant formation.

NOTATION

M = mass flux of particles, kg/m²s
r = radial coordinate, m
r_1 = primary jet radius, m
R^2 = statistical correlation coefficient
w = argon molar concentration, kg mole/m³
z = axial coordinate, m

Subscripts

1 = primary jet
c = center line
m = mean value
m = completed mixed value

ACKNOWLEDGMENT

This work was supported by the Electric Power Research Institute, Palo Alto, California, with Mr. John Dimmer as Project Officer, and by the U.S. Department of Energy, with Dr. Robert Wellek, Project Officer.

LITERATURE CITED

Beasley, T. F., D. M. Adams, and R. I. Vachon, "Secondary Peripheral Injection Effects on Axisymmetric Flow," *J. Spacecraft Rockets*, 7, No. 3, 347 (1970).

Durao, D., and J. H. Whitelaw, "Turbulent Mixing in the Developing Region of Coaxial Jets," *J. Fluid Eng.*, 95, 467 (1973).
Fejer, A. A., T. P. Torda, L. Boehman, K. N. Ghia, and W. G. Herman, "Research on Mixing of Coaxial Streams," *ARL 67-0058*, Ill. Inst. Technol., Chicago (Mar., 1967).
Harsha, P. T., "Free Turbulent Mixing: A Critical Evaluation of Theory and Experiments," *Rept. AEDC-TR-71-36*, Aero. Ind., Arnold A. F. Station, Tenn. (Feb., 1971).
Hedman, P. O., and L. D. Smoot, "Particle-Gas Dispersion Effects in Confined Coaxial Jets," *AIChE J.*, 21, 372 (1975).
Memmott, V. J., "Rates of Mixing of Particles and Gases in Confined Jets," M.S. thesis, Brigham Young Univ., Provo, Utah (Apr., 1977).
Skinner, F. D., R. W. Hanks, and L. D. Smoot, "A Facility for Study of Turbulent Mixing and Kinetic Processes in an Entrained Coal Gasifier," Paper No. 7655, Western States Section/Combustion Institute, La Jolla, Calif. (Fall, 1976).
Smoot, L. D., "Turbulent Mixing Coefficients for Compressible Coaxial Submerged and Coflowing Jets," *AIAA J.*, 14, 1699 (1976).
———, and L. D. Allred, "Particle and Gas Mixing Effects in Confined Nonparallel Coaxial Jets," *ibid.*, 13, 721 (1975).
Smoot, L. D., and L. A. Fort, "Confined Jet Mixing with Nonparallel Multiple-Port Injection," *ibid.*, 14, 419 (1976).
Smoot, L. D., and W. E. Purcell, "Model for Mixing of a Compressible Free Jet with a Moving Environment," *ibid.*, 5, 2044 (1967).
Stowell, D. E., and L. D. Smoot, "Turbulent Mixing Correlations in Free and Confined Jets," AIAA Paper No. 73-1194, AIAA/SAE 9th Propulsion Conference, Las Vegas, Nev. Nov. 5-7, 1973).
Thurgood, J. R., L. D. Smoot, and D. Rees, "A Facility to Study the Effects of Turbulent Mixing in Pulverized Coal Combustion," Paper No. 76-54, Western States Section/Combustion Institute, La Jolla, Calif. (Fall, 1976).
Tufts, L. W., and L. D. Smoot, "A Turbulent Mixing Coefficient Correlation for Coaxial Jets with and Without Secondary Flows," *J. Spacecraft Rockets*, 8, 1183 (1971).

Manuscript received June 17, 1977; revision received December 23, and accepted January 5, 1978.

Dispersion Measurement in Clogged Filter Beds: A Diagnostic Study on the Morphology of Particle Deposits

HEMANT PENDSE
CHI TIEN
R. RAJAGOPALAN
and
R. M. TURIAN

Department of Chemical Engineering and Materials Science
Syracuse University
Syracuse, New York 13210

The use of tracer dispersion measurements in conjunction with associated pressure drop data, as an indirect diagnostic technique for the determination of particle deposit morphology in deep-bed filters, was investigated. The dispersion measurements consisted of the injection of an electrolyte tracer pulse at the inlet and the monitoring of the tracer peak as it traveled down the bed, while the pressure drop data consisted of the axial pressure gradient histories as deposition took place. These data are interpreted using dispersion and pressure drop theories established on the basis of assumed models of deposit morphology. The validity of this technique was confirmed experimentally.

SCOPE

The development of an experimental procedure for the determination of the morphology of particle deposits in a clogged filter bed using a combination of tracer dispersion and pressure drop measurements is examined. In concession to the inherent difficulties associated with possible direct methods of ascertaining the nature of the deposited material in a practical filter bed, the method explored here is indirect and essentially inferential. The basic idea of the present diagnostic procedure is to develop pressure drop expressions corresponding to various assumed deposit morphologies. Thus, a quantitative description of the change of the bed structure in the clogged filter can be obtained from values of the pressure drop increase. Further, using the inferred data on the altered bed structure, calculations relating to the response of a tracer pulse injected at the bed inlet, and in particular those relating to the speed of travel of the tracer peak through the bed, are carried out. These calculated predictions are then compared with experimental tracer dispersion measurements. Poor agreement between prediction and experiment would mean that the original assumed deposit morphology is inappropriate, while satisfactory agreement would at least suggest that the basic model assumed for the distribution of deposited matter is plausible and a suitable candidate for further development. The work reported here consists of three parts: the analysis of the convective dispersion problem relating to the response of a tracer pulse injected into a clogged filter bed, the development of relationships between pressure drop increase and change in bed structure due to clogging corresponding to assumed deposit morphologies, and dispersion measurement in a clogged test filter resulting from the filtration of aqueous talc suspensions in order to confirm the validity of the technique.

R. Rajagopalan is with the Department of Chemical and Environmental Engineering, Rensselaer Polytechnic Institute, Troy, New York 12181.